Estimation of Sea Surface Temperature from Space

D. ANDING and R. KAUTH, Institute of Science and Technology, The University of Michigan, Ann Arbor, Michigan

Abstract

A procedure is derived for obtaining improved estimates of water surface temperature by means of spatially scanning space-borne systems which would perform simultaneous radiometric measurements in two wavelength intervals in the thermal infrared atmospheric-window spectral regions. The procedure should reduce errors in the estimate of water surface temperature caused by haze and water vapor effects from approximately ±2.0°C to approximately ±0.15°C.

Introduction

A knowledge of the distribution of water surface temperature over all bodies of water on the earth's surface is of significant importance to a number of scientific communities. Such information would be particularly useful in locating various species of fish, in spatially mapping ocean and lake currents, and in estimating the exchange of thermal energy between the water surface and the atmosphere. In general, the more precise the knowledge of the temperature distribution, the more useful are the data. However, the greater the precision desired, the higher is the cost of achieving that objective. Stevenson (1970), a representative of the scientific community, has stated that estimates of relative temperature within ±1°C at a spatial resolution of approximately 1 km would be satisfactory. Another requirement of the scientific community is that the time period between the collection of the data and its dissemination in a useful form be of the order of days. In essence, an accurate near real-time synoptic view of the earth's water is desired.

Although such an objective could be satisfied in a number of ways, a feasible approach would be to utilize a spatially scanning space-borne system which includes a computerized data-reduction technique to facilitate rapid conversion of the measured data into a usable form, such as water surface temperature maps. Fortunately, most of the knowledge required to design such a system is presently available from the results of past analysis and measurement programs. In particular, spatially scanning space-borne systems have been flown, such as the Nimbus III medium-resolution infrared radiometer (MRIR), which had the capability of providing estimates of water surface temperature on a global basis. However, since these systems did not have the capability of compensating for the effects of the atmosphere, temperature estimates with errors of the order of ±2°C were the best that could be obtained. Also, these systems had a ground resolution greater than 6 km and were not designed for rapid, automatic data reduction. The problem is to determine the system modifications required to satisfy the stated objectives. The most important modification is the incorporation of techniques to compensate for atmospheric effects in order to obtain improved estimates of water surface temperature. This paper presents and discusses a technique for achieving this objective.

Theoretical basis of remote Sea Temperature Measurement at Thermal Infrared Wavelengths

The spectral radiance emitted by a greybody at wavelength λ is given by

$$L_\lambda^{\,g} = \epsilon(\lambda) L_\lambda^{\,b}(T) \qquad (1)$$

where $\epsilon(\lambda)$ is the spectral emissivity of the greybody, and $L_\lambda^{\,b}(T)$ is the radiance emitted by a blackbody. The latter is represented as

$$L_\lambda^{\,b}(T) = \frac{2c^2h}{\lambda^5\left[(\exp hc/\lambda kT) - 1\right]} \qquad (2)$$

where T is the temperature of the blackbody, c is the velocity of light, h is Planck's constant, k is Boltzmann's constant, and λ is the wavelength.

It is clear from these expressions that, if the emissivity is known, the greybody temperature can be determined by measuring the emitted spectral radiance and inverting equation (1). The application of such a measurement procedure in determining the temperature of a water surface exposed to the atmosphere is more complex. The spectral emissivity of a sea surface has a maximum value of approximately 0.98, which occurs near 11 μm. Consequently, as one attempts to measure the emitted radiation, some sky radiation is reflected from the water surface and collected by the infrared sensor. Also, since water does not become opaque to infrared radiation at thermal wavelengths until a depth of approximately 0.10 mm, some of the measured radiation emanates from water below the surface, which generally has a slightly different temperature. Therefore the temperature derived from a measurement of the radiance at the surface is the temperature of a greybody (whose emissivity is equal to the emissivity of the water surface) that yields an equivalent value of radiance (i.e., the "equivalent greybody temperature"). It is different from the actual surface temperature, the degree of difference depending on the magnitude of the reflected radiation and the temperature gradient near the surface.

The present analysis is not concerned with the relationship between the equivalent greybody temperature and the actual temperature, however, but only with the effect of the atmosphere on the equivalent greybody temperature derived from a radiometric measurement performed at satellite altitudes. Therefore all future references to water surface temperature denote the equivalent greybody temperature that would be derived from a radiance measurement at the surface.

Effect of the Atmosphere on Measured Radiance

Before reaching a space-borne sensor, the spectral radiance emanating from the water surface is attenuated by atmospheric constituents, such as clouds, haze, and absorbing gases. These atmospheric constituents also emit and scatter radiant energy which contributes to the total signal received by the sensor. The central problem in measuring accurately the water surface temperature from space lies in determining the extent to which such effects can be observed and compensated.

The atmosphere may be free of clouds or may contain clouds which are either opaque or semitransparent to the surface radiation. If the field of view of a measuring instrument is completely filled with an opaque cloud, no radiation from the water surface reaches the sensor, and a water surface temperature determination is impossible. However, if the surface is only

Remote Sensing of Environment 1 (1970), 217–220

partially obscured by a cloud or completely obscured by a semi-transparent cloud, a surface temperature estimate can be made. The optimum technique for detecting the presence of clouds and for making estimates of water temperature when the field of view contains clouds will be the subject of a forthcoming paper. This paper considers only the special case of atmospheres containing normal molecular constituents and haze.

In a clear atmosphere the spectral radiance leaving the top of the atmosphere is the sum of two sources of radiation: (i) the radiance from the water surface, as attenuated by the infrared-active molecules (H_2O, CO_2, O_3, CH_4, and N_2O) and atmospheric haze, and (ii) the radiance emitted by these atmospheric constituents. Mathematically, this spectral radiance, L_λ, is given by

$$L_\lambda = L_\lambda^g(T)\tau(\lambda) + L_\lambda^a \qquad (3)$$

where $L_\lambda^g(T)$ is the equivalent greybody radiance at the water surface, $\tau(\lambda)$ the atmospheric spectral transmittance, T the greybody temperature, and L_λ^a is the spectral radiance emitted by the atmosphere.

To demonstrate the magnitude of the effect of atmospheric absorption and emission on the spectral radiance leaving the top of the atmosphere, consider the radiance spectra given in Fig. 1. The solid curve is the spectral radiance from a water surface with a temperature of 290°K, as viewed from 100 km through a typical noncloudy atmosphere at an angle of 60° with the nadir. The dotted curves designate the spectral radiance that would be observed in the absence of an intervening atmosphere for water temperatures of 290°K and 285°K.[1] The spectral regions in which the effect of the atmosphere is the greatest (i.e., near 6.3 μm, 9.6 μm, and 15 μm) correspond respectively to the molecular absorption bands of water vapor, ozone, and carbon dioxide. The atmosphere has a lesser effect between these absorption bands, in the so-called atmospheric windows, the minimum effect occurring in the vicinity of 11 μm. However, even in this clearest atmospheric window, a temperature approximately 2°C less than the surface temperature would be inferred from space-borne radiance measurements if the effect of the atmosphere were neglected.

The difference between the temperature derived from space-borne measurements and the water surface temperature depends both on the distribution of atmospheric water vapor and temperature and on the nadir viewing angle. For nadir angles corresponding to near-horizon viewing and for very moist atmospheres, the spectral radiance at 11 μm would correspond to temperatures approximately 4°C cooler than the surface temperature. Even at near-nadir viewing through relatively dry, clear atmospheres, the temperature at 11 μm would be approximately 1°C cooler than the surface temperature. Therefore estimates of the water surface temperature within ± 1°C can be achieved only by correcting for the effects of atmospheric absorption and emission. A procedure devised to compensate for these effects is a simple application of multiband remote sensing techniques requiring simultaneous measurement of the radiance in two specially chosen wavelength regions, one in each of the two atmospheric windows (i.e., near 9.0 μm and 11 μm).

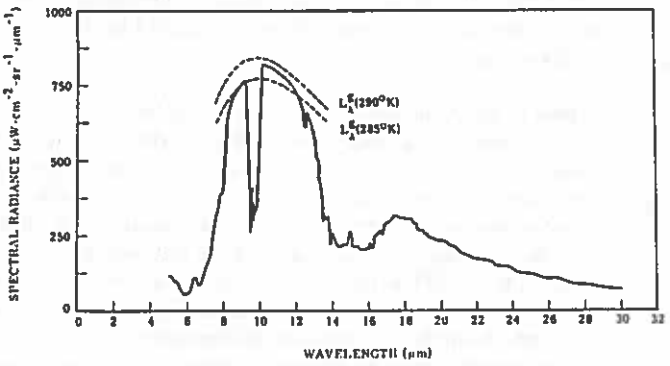

Fig. 1. Spectral radiance at 100-km altitude for a water surface temperature of 290°K. Nadir viewing angle = 60°.

Compensation of Atmospheric Effects with a System Utilizing Two Spectral Bands

In the two window regions, 7–9.5 μm and 10–12 μm, the only atmospheric constituent which significantly absorbs and emits radiation is water vapor, the absorption primarily resulting from the far wings of the intense spectral absorption lines in the 6.3-μm absorption band and those in the rotational water band (which begins to absorb strongly beyond 15 μm). The absorption near 9 μm is greater than that near 11 μm; therefore the temperature inferred from radiance measurements near 9 μm is less than that inferred from measurements near 11 μm (Fig. 1). Since the physical process which causes the absorption and the atmospheric emission in both window regions is the same, with the effect near 9 μm simply a slight magnification of the effect near 11 μm, a simultaneous measurement of the radiance in each window region should provide the necessary data to estimate the magnitude of water vapor absorption and emission. The problem involved (i) establishing the existence of two or more such spectral bands, and (ii) specifying the bands which would yield the optimum results.

The first step in the analysis was to obtain the relationship between the spectral radiance leaving the top of the atmosphere and the altitude distribution of water vapor and atmospheric temperature. Second, by use of this relationship, the existence of two spectral bands which would provide the necessary data to estimate the magnitude of water vapor absorption and emission was established. Finally, the optimum spectral bands for satisfying the stated objectives were selected.

Because of the complex relationship between the spectral radiance leaving the top of the atmosphere and the distribution of atmospheric water vapor and temperature, the relationship was empirically established by calculating the spectral radiance at 100-km altitude as a function of nadir viewing angle and water surface temperature for a number of different atmospheric water vapor and temperature distributions. An existing spectral radiance computer program, described by Anding and Kauth (1969), was used in these calculations. This computer program has the capability of calculating the spectral radiance from 5 to 30 μm, including the effects of water vapor, ozone, carbon dioxide, methane, nitrous oxide, and haze. Calculations can be performed for any nadir viewing angle and any distribution of atmospheric parameters. Since this analysis was concerned only with the effect of the atmosphere on the spectral radiance in the atmospheric window spectral regions, all atmospheric gas concentrations were held constant at representative average values, and water vapor and temperature were varied over a range of values. The actual temperature and water vapor altitude profiles used in these calculations are presented, respectively, in Figs. 2 and 3. They are representative of extreme conditions for summer and winter seasons for an at-

[1] For this case, $\tau(\lambda) = 1.0$ and $L_\lambda^a = 0$. Therefore the observed radiances are respectively given by $L_\lambda = L_\lambda^g$ (290°K) and $L_\lambda = L_\lambda^g$ (285°K).

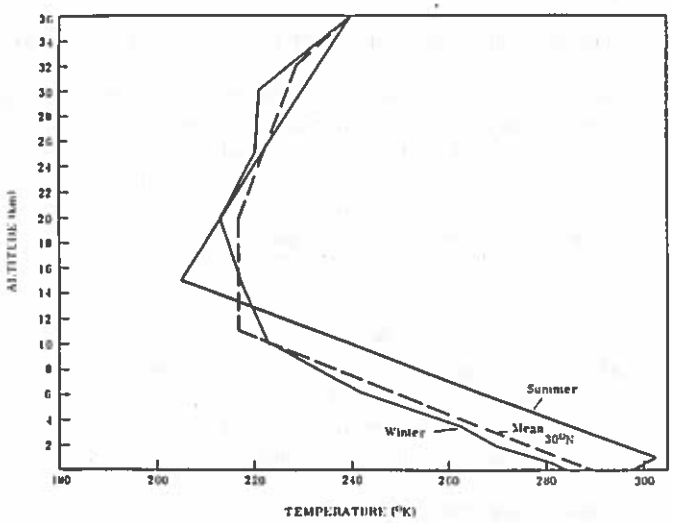

Fig. 2. Temperature profiles.

mosphere at latitude 30°N. Although these profiles do not bound all atmospheric conditions which could exist over the entire globe, they do encompass a sufficient range of values to determine the desired relationship between spectral radiance and atmospheric state. From these water vapor and temperature data, five model atmospheres were obtained by selecting five pairs of temperature and water profiles as shown in Table I.

Table I

Model atmospheric name	Temperature profile	Water profile
Summer wet	Summer	Summer wet
Summer dry	Summer	Summer dry
Winter wet	Winter	Winter wet
Winter dry	Winter	Winter dry
Mean, 30°N	Mean	Mean

For each model atmosphere, spectral radiance calculations were performed for three nadir angles (0°, 60°, 75°) and five water surface temperatures (280°, 285°, 290°, 295°, and 300°K). Thus a total of 75 spectra were calculated. The values of spectral emissivity of the water surface and the degree of dependence of emissivity on nadir viewing angle were taken from the work of Buettner and Kern (1965).

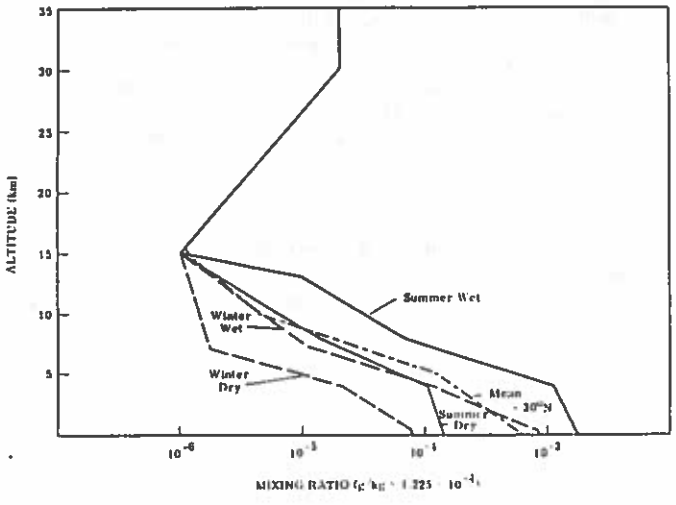

Fig. 3. Water vapour profiles.

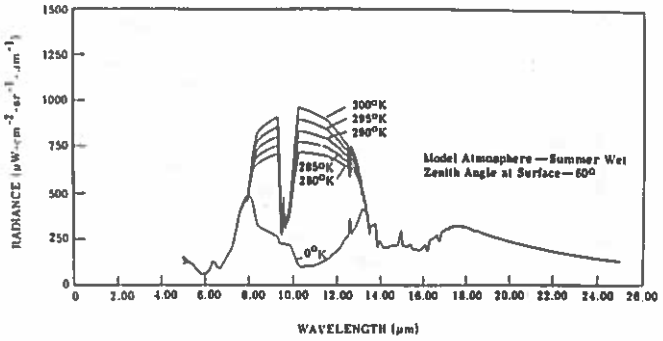

Fig. 4. Upwelling spectral radiance at 100 km with sea surface temperature as a parameter.

An example of the spectral radiance data calculated is given in Fig. 4. The data represent the upwelling spectral radiance at 100 km at a nadir angle of 60° for a summer-wet atmosphere and six water surface temperatures. Each of the radiance spectra is the radiance emitted by a greybody at a temperature equal to the water-surface temperature, modified by the molecular absorption and emission bands of the atmosphere. The 0°K surface temperature was included to reveal the magnitude of the spectral radiance emanating only from the atmosphere. Near the center of the intense absorbing regions (i.e., the 6.3-μm H_2O band and the 15-μm CO_2 band), the spectra are the same for all water surface temperatures because the atmosphere is opaque in these spectral regions.

The validity of the use of the calculated spectra for the present analysis was established by comparing calculations of spectral radiance with data obtained with the Nimbus III Infrared Interferometer Spectrometer (IRIS) for known atmospheric conditions. A representative result of such comparisons is shown in Fig. 5. Although in some spectral regions minor differences are observable, they are negligible in the atmospheric-window regions.

The relationship between the spectral radiance near 9 μm and that near 11 μm was empirically derived from the calculated spectra. Each of the calculated radiance spectra was spectrally smoothed to various resolutions, each resolution element being narrow enough to remain within an atmospheric window but broad enough to accept sufficient radiant power when implementing a satellite-borne scanning radiometer. Specifically, the spectra were smoothed to three different resolutions, 0.5, 1.0, and 1.5 μm, and the radiance values were obtained every 0.1 μm throughout each window region. From the smoothed data, all possible pairs of radiance values were selected, one value from the 9-μm window and one from the 11-μm window. For each pair of values, one value of radiance was

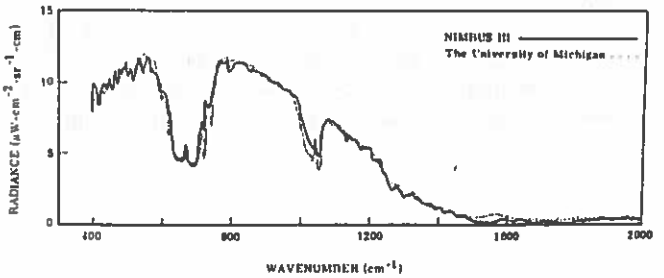

Fig. 5. Comparison of the University of Michigan calculations and the satellite-borne measurements.

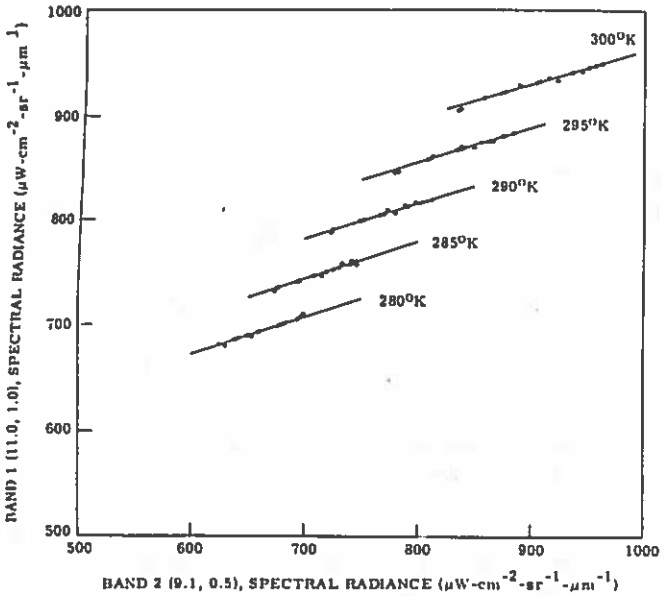

Fig. 6. Spectral radiance in band 1 vs that in band 2 as a function of atmospheric state. Parameters = zenith angle at surface and sea surface temperature.

plotted versus the other, each data point corresponding to a single atmospheric state, a particular nadir viewing angle, and a given water surface temperature. An example of one such plot is shown in Fig. 6. Each spectral band is denoted by its center wavelength and spectral bandpass (λ_c, $\Delta\lambda$). The values for the band pair represented are, respectively, (9.1, 0.5) and (11.0, 1.0). The radiance values for each temperature are well represented by straight lines, which were chosen to minimize the rms orthogonal error. For many of the band pairs, nonlinearities were observed and, in most cases, the scatter in the data points was extremely large. The result shown is for the band pair which gave the best results in regard to linearity and minimum scatter.

The interpretation of the results obtained is straightforward. Given the radiance in one spectral band and the water surface temperature, the spectral radiance in the other band is accurately predictable. In essence, the amount of atmospheric absorption and emission can be predicted. Conversely, given the radiance in each of the two spectral bands for any arbitrary distribution of atmospheric water vapor and temperature, the water surface temperature can be accurately estimated. The existence of a band pair showing linearly related radiance values is not surprising. Since the physical process which causes the absorption and the atmospheric emission in both spectral regions is the same, with the effect in the 9.1-μm band simply a slight magnification of that near 11 μm, a high correlation between the radiance values was expected. The linearity results from the fact that the atmospheric absorption and emission in both spectral regions are small and well represented by linear functions.

The unique feature of the result is that the series of nearly parallel, equally spaced lines provides a basis for a simple data-reduction algorithm, which is but a linear interpolation between the equitemperature lines. Had the relationship between the two channel radiance values been defined by a more complicated function, the two channel measurements could still provide accurate estimates of water surface temperature. The data-reduction algorithm would, however, be more complex.

To demonstrate the magnitude of the errors resulting from the use of this algorithm to estimate the water surface temperature, a surface temperature was calculated for each of the 75 radiance pairs plotted in Fig. 6. For each data point the difference between the estimated temperature T_i and the water surface temperature T_s was calculated. The rms error E in the estimated surface temperatures was then calculated by the formula

$$E = \sqrt{\frac{1}{N}\sum_{i=1}^{N}(T_i - T_s)^2} \qquad (4)$$

where N is the total number of data points (here $N=75$). For the band pair given in Fig. 6, the error was determined to be ± 0.15°C, a significant improvement over an error of ± 2°C, the best obtainable with a single-band system.

Summary and Conclusions

This analysis has demonstrated that, by performing radiometric measurements simultaneously in two spectral bands located in the thermal infrared atmospheric-window regions, the effects of water vapor absorption and emission can be almost completely compenated without the aid of meteorological support data. The ± 0.15°C error in the temperature estimate resulting from atmospheric effects, coupled with a noise equivalent temperature of approximately 0.4°C (representative of state-of-the-art systems), indicates that temperature estimates well within the stated objectives of ± 1.0°C are obtainable for non-cloudy atmospheres. By the use of additional spectral bands it is possible to indicate automatically the presence of clouds within the field of view and to estimate the water surface temperature in the presence of partial obscuration. The number of spectral bands, the band centers, and the bandwidths required to achieve this goal will be delineated in a forthcoming paper.

Acknowledgments

The authors gratefully acknowledge the contribution of Mr. Glen Larson of NASA-ERC in defining the objectives of this effort.

References

Anding, D., and R. Kauth (1969), Atmospheric modeling in the infrared spectral region: Atmospheric effects on multispectral sensing of sea-surface temperature from space, Report 2676-1-P, Willow Run Laboratories, Institute of Science and Technology, The University of Michigan, Ann Arbor, Michigan.

Buettner, K. J., and C. D. Kern (1965), The determination of infrared emissivities of terrestrial surfaces, *J. Geophys. Res.*, 70 (6).

Stevenson, R. E. (1970), Oceanographic applications and limitations of satellite remote sensors, *Bull. Am. Inst. Aeronaut. Astronaut.*, 7 (2).

Received July 27, 1970

The research described in this paper was performed under Contract No. NAS12-2117, sponsored by the Electronics Research Center, National Aeronautics and Space Administration.

REMOTE SENSING OF ENVIRONMENT 2, 165–169 (1972)

Comment on "Estimation of Sea Surface Temperature from Space" by D. Anding and R. Kauth

GEORGE A. MAUL

Physical Oceanography Laboratory, National Oceanic & Atmospheric Administration, Atlantic Oceanographic & Meteorological Laboratories, Miami, Florida 33130

MIRIAM SIDRAN*

N.S.F. Science Faculty Fellow, National Oceanic & Atmospheric Administration, Southeast Fisheries Center, Miami, Florida 33149

In the course of investigating the remote sensing of sea surface temperature with the NOAA 1 scanning radiometer, the calculations of Anding and Kauth (1970) were checked using the atmospheric transmissivity model of Davis and Viezee (1964). We found that according to this model, the 11.0 μm/9.1 μm band pair proposed by Anding and Kauth will not provide the information needed to compensate for water vapor in a cloud-free atmosphere, because the transmissivities in these bands due to water vapor are almost identical.

The model developed by Davis and Viezee uses analytic expressions for calculating the infrared transmissivity through water vapor and carbon dioxide. Coefficients for these expressions are tabulated in intervals of 25 cm^{-1} over the range 25–2150 cm^{-1}; the environmental variables are temperature, pressure, and amount of absorbing gas. The mean transmissivities are computed over finite spectral intervals, and this makes it possible to solve the radiative transfer equation in the form given by Craig (1965) for an absorbing, emitting, but nonscattering atmosphere. The validity of the model for the lower atmosphere has been established by Saunders (1970) and others.

Our calculations were carried out on the National Oceanic and Atmospheric Administration's computer facility at Suitland, Maryland. Input variables for the program were sea surface temperature, and atmospheric data in radiosonde format, i.e., temperature and relative humidity as a function of pressure. Amounts of absorbing gases along the path were calculated from the radiosonde data; the atmosphere-centimeters of carbon dioxide were calculated assuming that CO_2 is uniformly mixed 0.031 % by volume. The emissivity of the sea surface was assumed to be unity.

A vehicle altitude of 1200 km was chosen as being typical of a sun-synchronous orbit. The curvature of the earth was taken into account. (At this altitude and at a 60° nadir angle, the path length is 20 % longer than if the earth were assumed planar.) Transmissivities were calculated at one millibar intervals, from the surface up to one millibar (~48 km).

Anding and Kauth had plotted the calculated spectral radiance at 11.0 μm versus that at 9.1 μm (their Fig. 6) and had obtained a unique straight line for each surface temperature, thus correcting for water vapor effects. They found an rms error of 0.15°C in estimating sea surface temperature from this graph. As a first order check on these results, we did not attempt to use exactly the same band widths or central wave lengths. Instead, we plotted in Fig. 1 the spectral radiance at 912.5 cm^{-1} (10.96 μm) versus that at 1087.5 cm^{-1} (9.19 μm). Our calculations covered a wide range of sea surface temperatures (T_s) and geographically meaningful atmospheres (U.S. Standard Atmosphere Supplements, 1966), which are listed in Table I.

In contrast to the results of Anding and Kauth all points in Fig. 1 fall on the same straight line. An explanation of our results is found by examining the analytic expression used by Davis and Viezee in this region of the infrared spectrum,

$$\tau_\nu = \exp\left[-(k_\nu WP)^{a_\nu}\right],$$

where τ_ν is the transmissivity for the 25-cm^{-1} wave-number interval centered at wave number ν,

* On leave from New York Institute of Technology.

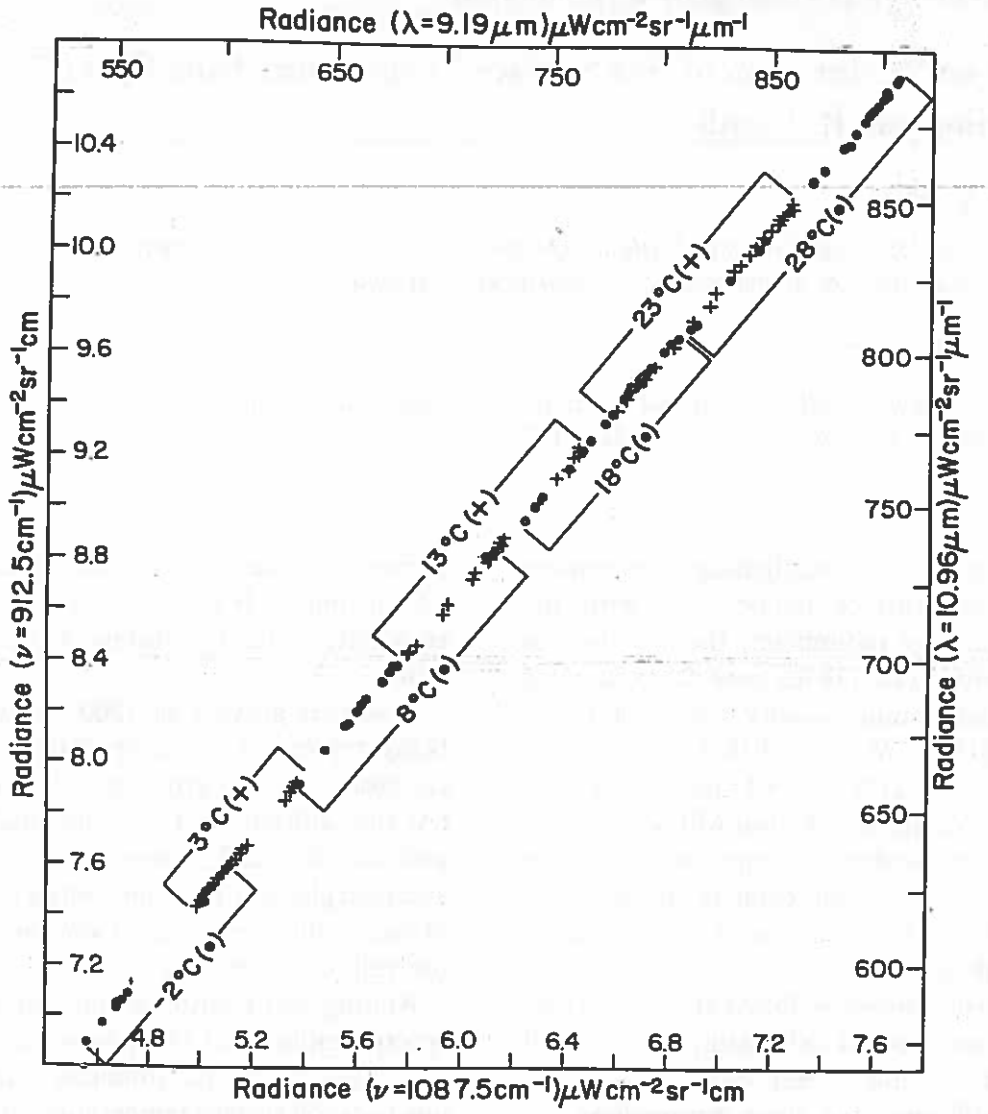

FIG. 1. Radiance at 912.5 cm^{-1} (10.96 μm) versus radiance at 1087.5 cm^{-1} (9.19 μm). Even degree values of T_s are dots; odd degrees are crosses. For each value of T_s the upwelling radiance was computed through three model atmospheres and for each 10° of nadir angle from 0° to 60°. The spectral radiances from different values of T_s overlay one another which does not allow a unique solution for atmospheric correction.

W is the amount of precipitable water vapor in cm, P is the ratio of *in situ* pressure to standard pressure, and k_ν and a_ν are constants. The values of k_ν and a_ν for the wave number interval 900–925 cm^{-1} are 0.095 and 0.885 respectively; for the interval 1075–1100 cm^{-1} they are 0.091 and 0.880 respectively. The near equality of these constants for each of these spectral bands means that the transmissivities due to water vapor are approximately equal.

To proceed with the explanation of our results, consider an atmosphere containing water vapor that absorbs but does not emit. Then the equation of radiative transfer in wavelength space reduces to

$$N_\lambda d\lambda = \tau_\lambda L_\lambda(T_s) d\lambda,$$

where N_λ is the radiance of wavelength λ, τ_λ is the transmissivity of the entire atmosphere, and $L_\lambda(T_s)$ is the blackbody radiance at the temperature T_s. The radiance (wavelength units) $L_{9.1\,\mu m}$ is nearly equal to $L_{11.0\,\mu m}$ for realistic ocean surface temperatures. Since $\tau_{9.1\,\mu m} \approx \tau_{11.0\,\mu m}$ then $N_{9.1\,\mu m} \approx N_{11.0\,\mu m}$ for all T_s. That is, a decrease in τ due only to H_2O, would decrease the radiance in both channels by about the same amount. Thus a plot of $N_{9.1\,\mu m}$ versus $N_{11.0\,\mu m}$ would yield one straight line (of slope about unity) for all T_s, and for all nadir angles and amounts of precipitable water. Emission by the atmosphere would change the slope somewhat, as in Fig. 1.

Davis and Viezee's transmissivity model was

TABLE I

Tabulation of the sea surface temperatures (T_s) and the model U.S. Standard Atmospheres used in the calculations. For each atmosphere/T_s pair are listed: The amount of precipitable centimeters of water vapor, the atmosphere-centimeters of carbon dioxide, the temperature departure ΔT ($\Delta T = T_s - T_c$ where T_c is the calculated equivalent blackbody temperature at the top of the air column) at nadir viewing for the 900–925 cm^{-1} spectral interval, and the surface air temperature (T_a).

T_s (°C)	Atmosphere	H_2O (pr.cm.)	CO_2 (at.-cm.)	ΔT (°C)	T_a (°C)
28°	15°N Annual	4.05	248.5	6.2	26.5
	30°N January	2.08	250.2	6.5	14.0
	30°N July	4.36	248.8	6.8	28.0
23°	30°N January	2.08	250.2	5.0	14.0
	30°N July	4.36	248.8	4.2	28.0
	45°N July	2.96	248.6	4.6	21.0
18°	30°N January	2.08	250.2	3.5	14.0
	45°N January	0.80	249.3	3.6	- 1.0
	45°N July	2.96	248.6	2.6	21.0
13°	45°N January	0.80	249.3	3.0	- 1.0
	45°N July	2.96	248.6	0.5	21.0
	60°N July	2.07	247.5	2.9	14.0
8°	45°N January	0.80	249.3	2.3	- 1.0
	45°N July	2.96	248.6	-1.6	21.0
	60°N July	2.07	247.5	1.3	14.0
3°	45°N January	0.80	249.3	1.6	- 1.0
	60°N January	0.36	248.2	1.5	-16.0
	60°N July	2.08	247.5	-0.3	14.0
-2°	45°N January	0.80	249.3	0.9	- 1.0
	60°N January	0.36	248.2	1.2	-16.0
	60°N July	2.08	247.5	-1.9	14.0

used to find line separation for different T_s. We retained the 912.5-cm^{-1} band as the basis of comparison, and plotted in Fig. 2 the radiance in this band versus that in the 1162.5-cm^{-1} (8.60-μm) band which is closer to the center of the water vapor absorption line. (For the 1150–1175-cm^{-1} interval, $k_\nu = 0.115$ and $a_\nu = 0.795$.) This band pair was the best compromise between maximum separation of T_s values and minimum scatter, according to our model. Our results are not as encouraging as those of Anding and Kauth; using their Eq. (4), the rms error in the estimated 28° surface temperature is 0.6°C. This is because each T_s line is really a family of closely spaced lines each corresponding to a different temperature-humidity profile.

At first, we tried to explain the discrepancy between our results and those of Anding and Kauth as due to the inclusion of ozone in their model. However, Kauth (1972, personal communication) was kind enough to show that this was not the case. We now believe that the discrepancy is due to the use of different transmissivity equations and that therefore both sets of results are model-dependent.

The expression used by Anding *et al.* (1971) for water vapor transmissivity (τ) is

$$\tau(\Delta\lambda) = \exp\left[-(W' \cdot K[\Delta\lambda])^{1/2}\right]$$

where $K(\Delta\lambda)$ is the spectral absorption coefficient and W' is the equivalent optical depth due to water vapor, given by

$$W' = \rho \int_0^R M \left[\frac{P}{P_0}\right]^2 \left[\frac{T_0}{T}\right]^{1.5} dr$$

where P is the atmospheric pressure (mm Hg), T is the atmospheric temperature (°K), r is the range (cm), ρ is the atmospheric density (g cm^{-3}), M is the mixing ratio (g H_2O/g air), P_0 is the

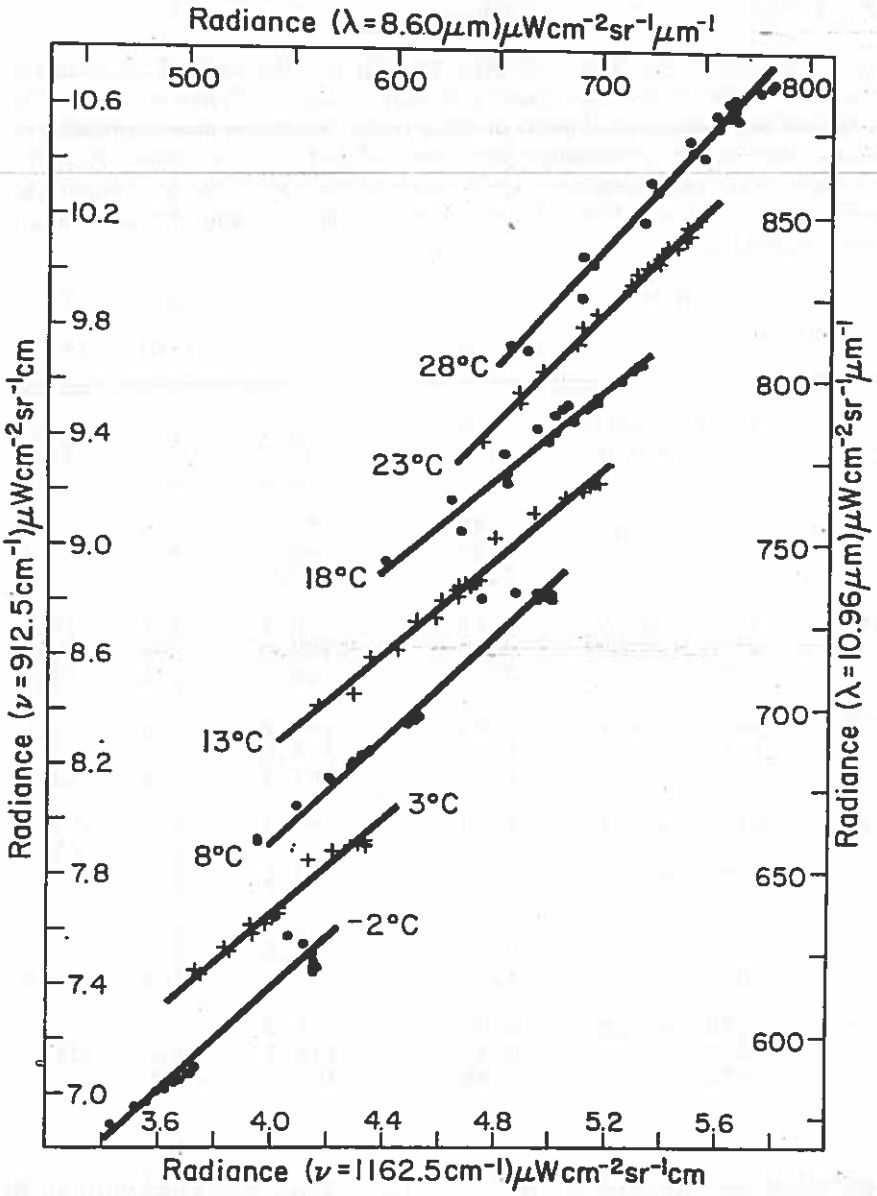

FIG. 2. Radiance at 912.5 cm^{-1} (10.96 μm) versus radiance at 1162.5 cm^{-1} (8.60 μm). Even degree values of T_s are dots; odd degrees are crosses. For each value of T_s, the upwelling radiance was computed through three model atmospheres and for each 10° of nadir angle from 0° to 60°. The straight line through each T_s family is the least-squares best fit. The lines were not constrained to pass through the point of no atmospheric effect although McMillin (1972, personal communication) suggests they should.

standard pressure and T_0 is the standard temperature. From their table of spectral absorption coefficients we estimate that $K(\Delta\lambda) = 2.72 \times 10^{-3}$ for the 900–925 cm^{-1} interval, and $K(\Delta\lambda) = 2.35 \times 10^{-2}$ for the 1075–1100 cm^{-1} interval. The large difference in $K(\Delta\lambda)$ is the reason for the success of Anding and Kauth's model. It causes the τ's to be unequal, and leads to the separation of lines in their Fig. 6.

We checked the transmissivities reported by several other investigators, and computed their ratios. From Taylor and Yates (1957, Fig. 8) we scaled a transmission ratio $\tau_{11.0}/\tau_{9.2} = 1.15$ for a horizontal path containing 1.37-cm precipitable water in an atmosphere very near NTP. For these same conditions, Anding and Kauth's equation yielded $\tau_{10.96}/\tau_{9.19} = 1.13$, and Davis and Viezee's expression gave $\tau_{912.5}/\tau_{1087.5} = 0.996$. Kondrat'ev *et al.* (1966) used an expression $\tau = \exp(-KW)$ where we estimate $K_{912.5} = 0.107$ and $K_{1087.5} = 0.090$; again for $W = 1.37$ cm, $\tau_{912.5}/\tau_{1087.5} = 0.977$. Finally we scaled a ratio $\tau_{11.0}/\tau_{9.2} = 0.975$ from Burch (1970, Fig. 3–1); this ratio is not for the same atmospheric con-

ditions, which we kept constant for the four previous comparisons. Thus, each model yielded a different ratio of τ for the two channels. From this we conclude that the degree of separation of lines of equal T_s depend on the transmissivity model used.

In conclusion, we feel that the family of solutions suggested by Anding and Kauth is a significant step in the remote sensing of the sea surface temperature. However, our calculations suggest that the separation of lines of different T_s depends on the transmissivity model employed. The Surface Composition Mapping Radiometer (originally designed for land use) to be flown on Nimbus E later this year, and the Sea Surface Temperature Imaging Radiometer proposed for the Earth Observatory Satellite both use the 11.0-μm/9.1-μm band pair. If the two channels have the limitations which our results would indicate, these instruments will not be useful for sea surface temperature measurements. In the meantime, we invite other investigators with different transmissivity models to check our results, and communicate their ideas on this subject.

References

Anding, D. and R. Kauth (1970), Estimation of sea surface temperature from space. *Remote Sensing* 1, 217–220.

Anding, D., R. Kauth, and R. Turner (1971), *Atmospheric effects on infrared multispectral sensing of sea surface temperature from space*, NASA CR-1858, Washington, D.C.

Burch, D. E. (1970), Semi-Annual Technical Report, *Investigation of the absorption of infrared radiation by atmospheric gases*, Philco-Ford Corp., Aeronutronic Division, Newport Beach, Calif., p. 5–2.

Craig, R. A. (1965), *The Upper Atmosphere, Meteorology and Physics*, Academic Press, New York.

Davis, P. A. and W. Viezee (1964), A model for computing infrared transmission through atmospheric water vapor and carbon dioxide, *J. Geophys. Res.* 69, 3785–3794.

Kondrat'ev, K. Ya., Kh. Yu. Niilisk, and R. Yu. Noorma (1966), The spectral distribution of the infrared radiation in the free atmosphere, *Izv. Atmos. & Ocean. Phys.* 2, 121–136.

Saunders, P. M. (1970), Corrections for airborne radiation thermometry, *J. Geophys. Res.* 75, 2796–7601.

Taylor, J. H. and H. W. Yates (1957), Atmospheric transmission in the infrared, *J. Opt. Soc. Am.* 47, 223–226.

U.S. Standard Atmosphere Supplements (1966). Superintendent of Documents, U.S. Government Printing Office, Washington, D.C.

Reply to the Comment by G. A. Maul and M. Sidran

D. ANDING and R. KAUTH

Institute of Science and Technology, University of Michigan, Ann Arbor, Michigan

We agree with the two major points made by Maul and Sidran. First, the water vapor transmission model used determines the spectral band pair which yields the best estimates of the sea surface temperature. Secondly, the spectral bands given in our paper of 1970 will not provide the necessary information to obtain improved estimates of sea temperature. This is not to imply that the two band concept is invalid, only that we have since found that the water vapor transmission model used in our previous analysis is not representative of reality. We have since altered the transmission model and obtained a new result which is presented herein.

Bignell (1970) published a comprehensive dissertation on the absorption by water vapor throughout the spectral region from 8 to 20 μm. Bignell demonstrated that three types of absorption occur in the window region: (a) that due to local lines, (b) a continuum caused by the wings of water vapor lines within the 6.3 μm band and the rotational water band which are pressure broadened by foreign gases, and (c) a continuum caused by water vapor lines which are self-broadened. The continuum absorption coefficient at temperature T, total pressure P, and water vapor partial pressure p, is given by

$$k(T,P,p) = k_1 P + k_2 p, \tag{1}$$

where

k_1 is the absorption coefficient for foreign broadening at unit total pressure;
k_2 is the absorption coefficient for self-broadening at unit water vapor partial pressure.

Values of k_1 and k_2 determined by Bignell (1970) are given in Fig. 1. Bignell's results clearly indicate that the water vapor model used in our previous analysis did not include the effects of absorption caused by self-broadening, which is

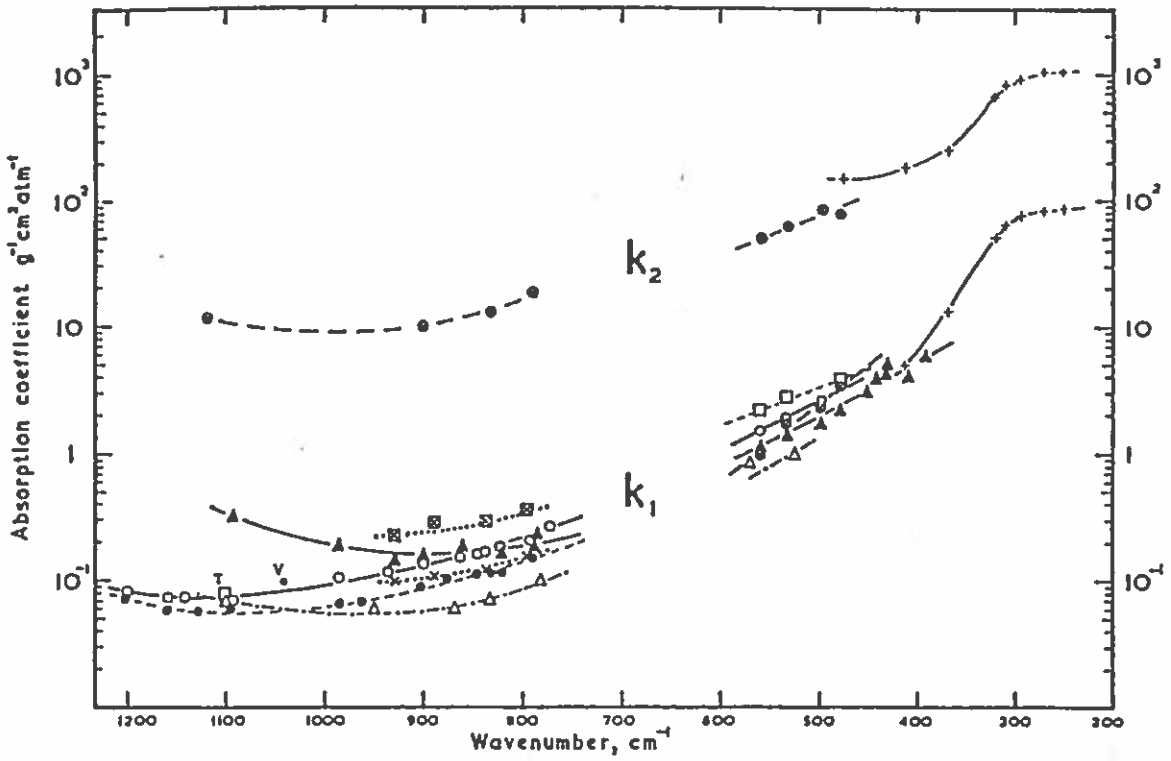

FIG. 1. Mass Absorption Coefficients (See Eq. 1) For The Foreign-Broadened (k_1) and Self-Broadened (k_2) Continuum. [Bignell]

significant for the atmospheric paths considered in the sea temperature study. This is also true of the model used by Maul and Sidran, but to a lesser extent. The latter model was based upon the data of Roach and Goody (1958), which included water vapor partial pressures at sea level as high as 15 mb. Therefore, some self-broadened-type absorption was reflected in the Roach and Goody data, but not at sufficient levels to define the value of k_2 accurately. It appears, therefore, that since neither our previous model, or the model used by Maul and Sidran, accurately represented the effects of self-broadening, neither result is acceptable.

In an effort to obtain a water vapor transmission model that provided for a better representation of reality, we have now used the data of Bignell for values of k_1 and k_2 in conjunction with the previously used values of Altshuler (1961) for local line absorption and have generated a new water vapor transmission model. Through the use of this new model and the statistical procedures described in our previous paper, a new two-channel pair was defined. The respective spectral bands are centered at 8.95 and 11.9 μm and have band widths of 0.5 and 1.0 μm, respectively. For each of these spectral bands, inband radiance calculations for the five model atmospheres defined in our previous paper, for each of five sea surface temperatures and three zenith angles were performed (75 cases in all).

Although there is more spread in the points than previously shown, the data are still reasonably well represented by straight nearly parallel lines. The standard error in the estimate of the sea surface temperature is now 1.59°K rather than 0.15°K shown previously. As shown in Fig. 2, this increased error arises primarily from two sources: (a) observations at large zenith angles without using zenith angle as a variable in the estimation rule, and, (b) large differences between the sea surface temperature and the temperature of the lower atmosphere. In Fig. 2, the ×'s are points for which the zenith angles are

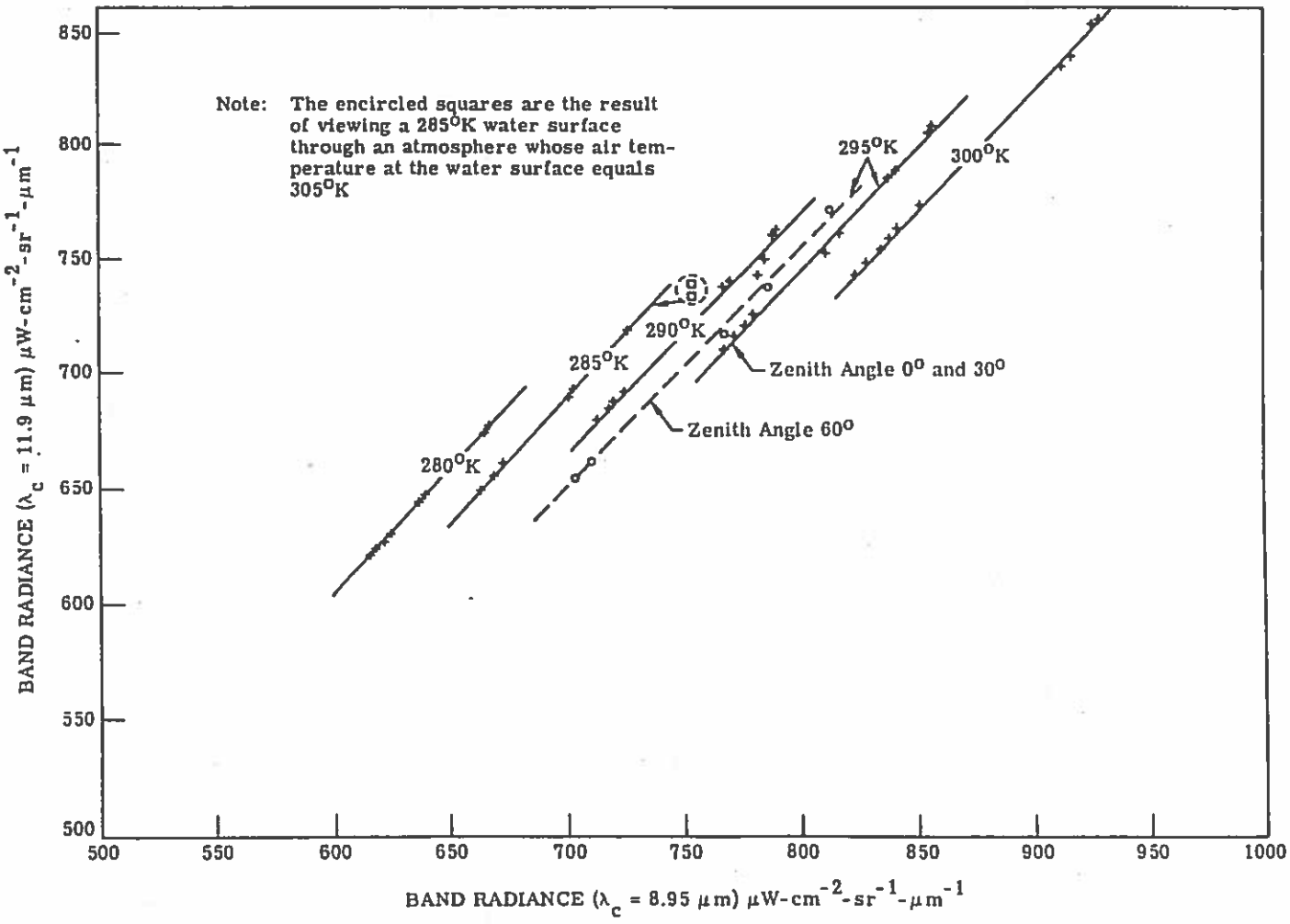

FIG. 2. Spectral Radiance in Band 1 vs. that in Band 2 as a Function of Atmospheric State. Parameters = zenith angle at Surface and Sea Surface Temperature.

0 and 30° and for which the difference between the surface temperature and atmosphere temperature at the surface is less than 10°K. If only this set of data points is included in the calculation, the standard error in the estimate of sea surface temperature is 0.45°K.

The circles in Fig. 2 are points for a zenith angle of 60°. They are shown for only one surface temperature, 295°K, to avoid cluttering the figure. Note that these points are well represented by a straight line, parallel to the others, but displaced. It is easy to see that if these points are accounted for by using a third observable, namely the zenith angle, in the estimation procedure the standard error can be reduced to near that for the 0 and 30° cases alone.

The squares in Fig. 2 are points for which the surface temperature is greater than 10°K different from the temperature of the atmosphere at the surface. Again, only one case, surface temperature equal to 285°K, is called out in the figure. In the calculation of standard error using all data these points were given equal weight with all others, while in the real world these points are quite unlikely to occur.

It is encouraging to note that even though the transmission models used by the authors are significantly different from each other (and also significantly different from that used by Maul and Sidran), the analysis performed on the data resulting from each model yielded two spectral bands (different for each case), which provided the necessary information to obtain a significant improvement in the estimate of the sea surface temperature over that obtainable from a single band measurement. It appears, therefore, that regardless of the spectral distribution of the absorption and emission of atmospheric water vapor in the spectral region of concern, a pair of spectral bands can be found which can achieve improved estimates of the sea surface temperature over that obtainable with a single band instrument. The problem is to determine the spectral bands which will yield the optimum results. If this is achieved through the use of simulated data, the credibility of the ir system depends upon the degree to which the water vapor transmission model represents reality. It would appear that the latest result is more credible than previous ones since it is based upon a water-vapor model which is in agreement with the latest accepted absorption data on self-broadened water vapor. The model does, however, lack verification and the results should not, therefore, be accepted as final.

The first spaceborne test of a two-channel procedure for estimating sea surface temperature will conceivably occur during the Skylab missions. The authors propose to estimate sea surface temperature for various two-channel pairs from data acquired by the S-191 interferometer spectrometer for sea surface test sites for which the sea surface temperature and atmospheric meteorology are accurately known. The test area (approximately one mile square) will be acquired 45 degrees forward of the spacecraft and tracked until the test area is 15 degrees aft. Approximately 60 spectra will be acquired from 6.2 to 15.5 μm and these data will be used in the analysis. Since variable path transmission will result from the varying nadir viewing angle, the data should be useful for water vapor transmission model verification, for testing the two-channel concept for sea surface temperature measurements, and for selection of a channel pair. In addition, the authors are currently working with personnel at Goddard Space Flight Center towards these objectives. The channel pair which is finally selected will be used on the Sea Surface Temperature Imaging Radiometer proposed for the Earth Observatory Satellite.

References

Bignell, K. J. (1970), *Quan. J. R. Met. Soc.* **96**, 390–403.

Roach, W. T. and R. M. Goody, (1958) *Quant. J. R. Met. Soc.* **84**, 319–333.

Burch, D. D., *Investigation of the Absorption of Infrared Radiation by Atmospheric Gases*, Philco-Ford Corporation, Aeronutronic Division, Newport Beach, Calif. Report No. U-4784 (January 1970).

Altshuler, T. L., *Infrared Transmission and Background Radiation by Clear Atmospheres*, General Electric Company, Missile And Space Vehicle Department, Philadelphia, Penn., Document No. 61SD199 (December 1961).